Mohsen Karimi[1,2,*]

Jose L. Diaz de Tuesta[1,2]

Carmem N. d. P. Gonçalves[2]

Helder T. Gomes[1,2]

Alírio E. Rodrigues[1]

José A. C. Silva[1,2,*]

Compost from Municipal Solid Wastes as a Source of Biochar for CO_2 Capture

Increasing greenhouse gas emissions contributing to the global climate change are a major concern of environmental protection. Developing adsorbents from low-cost and renewable resources is an attractive strategy. On the other hand, the high capacity of production rates of municipal solid waste, besides high methane emissions, is the origin of some eco-systemic challenges. The combination of the two environmental problems is considered by introducing the compost from a mechanical biological treatment of municipal solid wastes as a low-cost source of adsorbent for CO_2 capture. The obtained compost was thermally and chemically activated and the CO_2 adsorption capacities of prepared samples were evaluated. Samples prepared sequentially with sulfuric acid and heated at 800 °C and vice versa, respectively, had the highest uptake capacities and were comparable with commercial adsorbents.

Supporting Information available online

1 Introduction

1.1 Global Warming and CO_2 Capture

Global warming is one of the major concerns of mankind in the recent decades, which needs significant attempts to reduce the emission of greenhouse gases (GHGs) [1]. Among all GHGs, CO_2 plays the main role, contributing to several adverse effects on the ecosystem and environment, and if the current dangerous level of the GHGs is not controlled, it can face the life on this planet with serious challenges. The coal- and natural gas-fired power plants released 11.1 Gt of CO_2, nearly 30 % of the total global emissions in 2012 [2, 3]. In this way, the combustion of coal, also oil and natural gas industries including naphtha refineries [4, 5] and petrochemical complexes [6, 7], are the main industrial sources of CO_2 emissions [8, 9]. As consequence of these industrial activities, the CO_2 percentage exceeded 50 ppm in the atmosphere from the maximum allowable level in the pre-industrial period until now (280–400 ppm) [10, 11]. Thus, strict policies, better strategies, and more attention for capturing and sequestering CO_2 are required.

1.2 Solid Waste Management

Municipal solid waste (MSW) is a term usually referred to the unwanted or useless solid materials originating from the combined residential, industrial, and commercial activities in urban areas [12, 13]. The capacity of the MSW production was 2.01 billion metric tons per year in 2018, while this amount is expected to increase to around 3.40 billion metric tons per year in 2050 [14]. Also, it is estimated that ∼ 13.5 % of today's waste is recycled and 5.5 % is composted, while 40 % of worldwide generated waste is not properly managed. Therefore, rich countries, including the United States, Canada, and members of the European Union, having 16 % of global population, are responsible for more than 34 % of the world's waste [14]. To reduce the destructive effects of this huge amount of solid wastes, a large number of research activities have focused on the development of new waste management strategies. There are some main treatment techniques for solid wastes, such as employing extremely high temperatures [12], dumping on the land [15], and also applying biological processes to treat the wastes and produce compost, which is one of the most popular strategies [12, 15].

[1]Dr. Mohsen Karimi, Dr. Jose L. Diaz de Tuesta, Prof. Helder T. Gomes, Prof. Alírio E. Rodrigues, Prof. José A. C. Silva
mohsen.karimi@fe.up.pt
Laboratory of Separation and Reaction Engineering, Laboratory of Catalysis and Materials (LSRE/LCM), Department of Chemical Engineering, Faculty of Engineering, University of Porto, Rua Dr. Roberto Frias, S/N, 4099-002 Porto, Portugal.

[2]Dr. Mohsen Karimi, Dr. Jose L. Diaz de Tuesta, Carmem N. d. P. Gonçalves, Prof. Helder T. Gomes, Prof. José A. C. Silva
jsilva@ipb.pt
Centro de Investigação de Montanha (CIMO), Instituto Politécnico de Bragança, Campus de Santa Apolónia, 5300-253 Bragança, Portugal.

Wiley Online Library

1.3 Objective

A summary of main objectives of this study is given in Fig. 1. Based on the scopes of the carbon capture and storage (CCS) and the MSW management a novel strategy named integrated management of environment (IME) is proposed. In this way, the obtained compost in the mechanical biological treatment from the MSWs is considered as a low-cost source of adsorbent for CO_2 capture, which can be a promising technique for solid waste disposal.

2 Materials and Methods

2.1 Materials and Chemicals

In this work, the compost was supplied from a municipal solid waste management company (Resíduos do Nordeste, EIM, Portugal), after maturation of the digested side stream resulting from anaerobic digestion of the organic fraction of undifferentiated MSW sorted at the mechanical and biological treatment unit. Sulfuric acid (96–98 wt %) was obtained from Riedel-de-Haën. CO_2 and helium were supplied by Air Liquide, with purities of 99.98 % and 99.95 %, respectively.

2.2 Compost Preparation

The composts were obtained under the controlled aerobic decomposition of MSWs by the operation of microorganisms and small invertebrates. The rate of compost formation was adjusted by temperature, supplied moisture, and percentage of air in the reactor. Among all factors, the C/N ratio is the main one to prepare efficiently compost from the MSWs because carbon supplies the required energy for the microorganisms, while the nitrogen supports the growth of some available proteins.

The temperature is the other operational condition which should be controlled during the decomposition process. The desirable range of temperature is 50–60 °C, the optimum being 60 °C. Finally, the air should be adjusted to supply the required oxygen in the aeration step. More details about this process can be found in [15]. The simple schematic of this process is depicted in Fig. 2. The supplied composts are characterized in Tab. 1.

2.3 Activation Techniques

A summary of the activation procedure of different samples is illustrated in Fig. 3. In addition, a detailed description of this procedure is reported in Sect. S1 in the Supporting Information.

2.4 Characterization of Adsorbents

The elemental composition was quantified on a Carlo Erba EA 1108 Elemental Analyzer to determine the C, H, N, and S content of each prepared sample. Thermogravimetric analysis (TGA) was performed using a Netzsch STA 409 PC equipment under oxidative atmosphere. For that purpose, the samples were heated under air atmosphere condition from 323 K to 1273 K at 10 K min^{-1}.

The analysis of N_2 adsorption-desorption isotherms at 77 K was performed with a Quantachrome NOVA 4200e adsorption analyzer to detect the textural properties of the prepared samples. The Brunauer-Emmett-Teller (BET)-specific surface area (S_{BET})[1] was calculated by the BET method [16]. The external surface area (S_{ext}) and the micropore volume (V_{Mic}) were measured by applying the t-method [17] and employing the ASTM standard D-6556-01 to calculate the thickness (t). Then, the microporous surface area (S_{Mic}) was calculated by subtracting the S_{ext} from S_{BET}. Also, the approximation $W_{Mic} = 4\,V_{Mic}/S_{Mic}$ was considered to determine the average pore width (W_{Mic}). In addition, the total pore volume (V_{Total}) was considered at $p/p^0 = 0.98$.

2.5 Breakthrough Experiments

In order to evaluate the uptake capacities of the prepared samples for CO_2 capture, breakthrough experiments were performed in a fixed-bed adsorption unit built at our laboratory LSRE-LCM, which is illustrated in Fig. 4. In order to perform the adsorption experiments, in the first step an adsorption
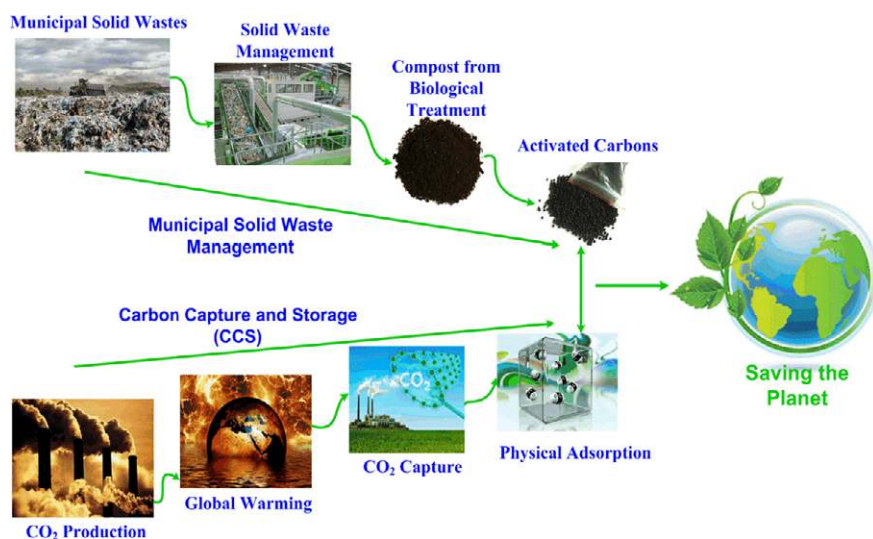

Figure 1. Integrated management of environment (IME) by CO_2 capture using materials developed from the municipal solid wastes.

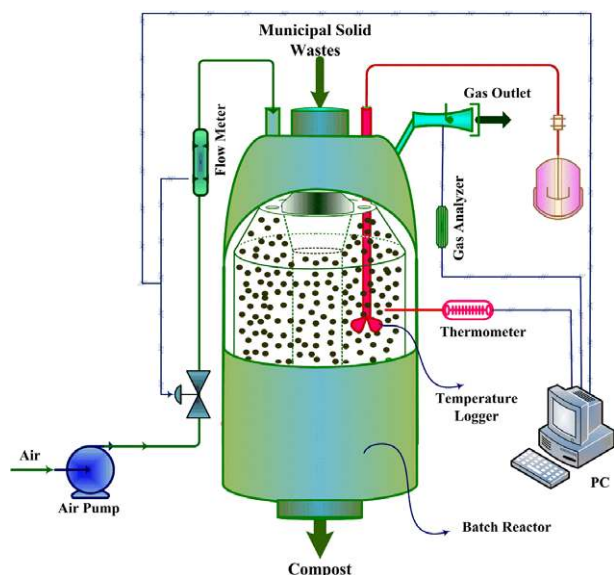1) List of symbols at the end of the paper.

Figure 2. Scheme of the digestive process to obtain biogas and prepare compost.

Table 1. Characterization of compost material derived from municipal solid waste based on dry conditions.

Parameter	Value
Moisture [%]	29.6
Organic matter [%]	48.8
C [%]	27.1
N [%]	1.3
P_2O_5 [%]	1.1
K_2O [%]	1.4
Ca [%]	4.9
Mg [%]	0.8
S [%]	0.6
B [%]	0.0043
Cd [%]	9×10^{-5}
Cr [%]	0.013
Cu [%]	0.021
Hg [%]	4×10^{-5}
Ni [%]	0.0049
Pb [%]	0.011
Zn [%]	0.045
Anthropogenic inert [%]	0.7
Escherichia coli [g^{-1}]	460
Density [$kg\,dm^{-3}$]	0.45
Electric conductivity [$mS\,cm^{-1}$]	2.5
pH [–]	8.0

column is filled with adsorbents. Then, the preparation procedure is accomplished by passing the hot career gas (helium) in the column for 12 h to remove impurities and moisture. After that, the adsorption process is initiated by introducing the adsorbate gas and carrier gas to the system. In this step, the system is analyzed continuously by measuring the mass flow rate at the output of the column with a thermal conductivity detector (TCD). Finally, after reaching the saturation conditions, the regeneration process (desorption) is started by switching the gas flow rate to the career gas to desorb the adsorbed CO_2 on the bed. More details about this unit can be found in our previous study [18].

After gathering the TCD results, a mass balance was considered on the adsorption bed to determine the uptake capacity of sorbents as follows:

$$Q_{CO_2} = \frac{1}{m_{adsorbent}} \left[\int_0^{t_s} \left(F_{CO_{2,in}} - F_{CO_{2,out}} \right) dt - \frac{y_{CO_2,feed} P_b \varepsilon_T V_b}{Z R_g T_b} - \frac{y_{CO_2,feed} P_b V_d}{Z R_g T_b} \right] \tag{1}$$
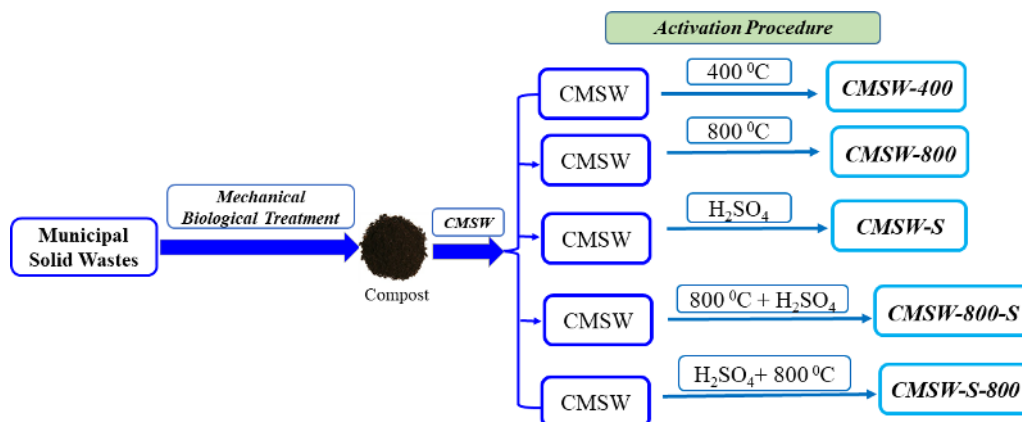

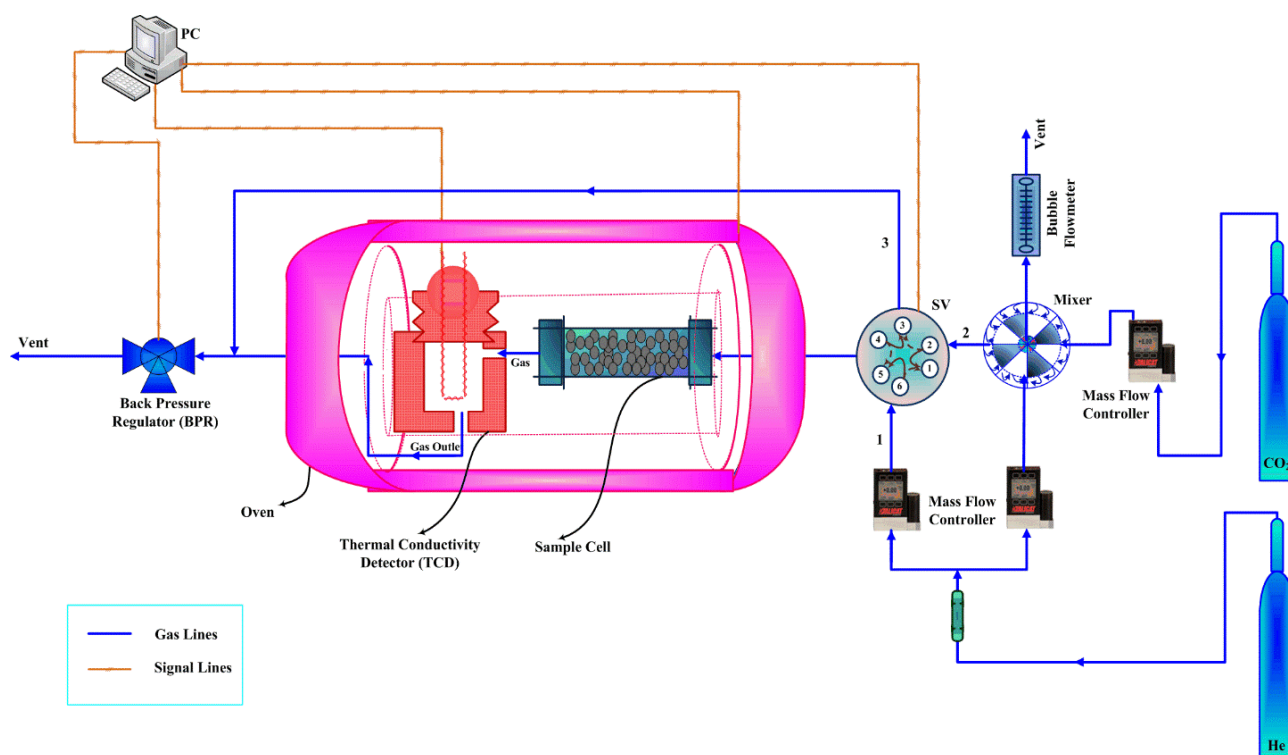**Figure 3.** Scheme of activation procedure of the different proposed samples.

Figure 4. Experimental setup used to measure the adsorption equilibrium of prepared samples.

Here, t_s is the saturation time of the bed and ε_T is the total porosity of the bed, which is determined by Eq. (2) [19]:

$$\varepsilon_T = \varepsilon_b + (1 - \varepsilon_b)\varepsilon_p \qquad (2)$$

Where ε_p is the particle porosity and ε_b is the packed bed porosity. More details about the breakthrough unit and operational conditions are presented in Tab. 2.

Table 2. Specific properties and operating conditions of breakthrough apparatus.

	CMSW-400	CMSW-800	CMSW-S	CMSW-800-S	CMSW-S-800
Bed characteristics					
Bed inner diameter [cm]	0.46				
Bed length [cm]	10				
Wall thickness [cm]	0.089				
Total parameters of experiments					
Mass of sample [g]	~0.6	~0.6	~0.6	~0.6	~0.6
Ambient pressure [bar]	1	1	1	1	1
Ambient temperature [K]	293.75	295.55	294.85	295.25	293.05
CO_2 flow rate [mL min^{-1}]	~10	~10	~10	~10	~10
Helium flow rate [mL min^{-1}]	~9	~9	~9	~9	~9
Particle sizes [μm]	53–106	53–106	53–106	53–106	53–106
Operating conditions					
Temperature [°C]	40	40	40	40	40
Total pressure [bar]	1–5	1–5	1–5	1–5	1–5

3 Modeling and Simulation

3.1 Breakthrough Modeling

In order to scale up the adsorption system, the analysis of the adsorption equilibrium data is required to estimate the adsorption capacities of the adsorbents. In this study, the Langmuir model, as the most popular model to describe monolayer adsorption processes, was applied to evaluate the obtained experimental data [20, 21]. In this model, the R^2 is considered to determine the accuracy of the fitted model to the experimental values. The Langmuir model is defined as:

$$Q_e = \frac{Q_m K_L P_{CO_2}}{1 + K_L P_{CO_2}} \tag{3}$$

Here, K_L as the Langmuir adsorption constant, determines the strength of created bonds between the adsorbate molecules and adsorbents, which can be described by:

$$K_L = \frac{\alpha \exp(\Delta H / R_g T)}{k_{d\infty} \sqrt{2\pi M R_g T}} = K_\infty \exp(\Delta H / R_g T) \tag{4}$$

$$K_\infty = \frac{\alpha}{k_{d\infty} \sqrt{2\pi M R_g T}} \tag{5}$$

where ΔH is the heat of adsorption, α denotes the sticking coefficient, T is the temperature, and M is the molecular weight. In addition, R^2 is calculated by:

$$R^2 = 1 - \frac{\sum_{i=1}^{n}(y_i - f_i)^2}{\sum_{i=1}^{n}(y_i - \bar{y})^2} \tag{6}$$

$$\bar{y} = \frac{1}{n}\sum_{i=1}^{n} y_i \tag{7}$$

where y_i and f_i are the experimental and predicted vales, respectively.

3.2 Response Surface Methodology

Response surface methodology (RSM) is a combination of statistical and mathematical methods which is employed to design experiments, develop models, determine the parameter interactions, and also to find the optimal values of independent variables [22]. Among the different methods of RSM, the central composite design (CCD) is the most popular one [9, 22]. In this way, the obtained experimental values for the mathematical-statistical treatment are fitted to a quadratic equation as follows:

$$Y = \beta_0 + \sum_{i=1}^{n} \beta_i x_i + \sum_{i=1}^{n} \beta_{ii} x_i^2 + \sum_{i=1}^{n} \sum_{j=i+1}^{n} \beta_{ij} x_i x_j + \varepsilon \tag{8}$$

where Y is the response value, x_i and x_j indicate the independent variables, which are defined in the range of [0–1] as coded

values of model factors, β_i and β_j illustrate the linear coefficients of independent variables, while β_{ii} or β_{jj} display the quadratic coefficients of the model, and β_0 is the intercept coefficient. In addition, the interaction effects between the independent variables is defined by β_{ij}.

In this equation, the residual error is calculated by ε. Then, by employing the least square method and multiple regression analysis, the mentioned coefficients are computed contributing to a general correlation. In this way, the regression analysis of variance (ANOVA) of the designed model is performed by the statistical evaluation of results to get a significant model for the adsorption process. Then, the model lack-of-fit, which determines the variations of the data around the fitted model, should be considered, and if the model does not fit the data very well, the lack-of-fit will be significant and contributes to an undesirable model [23].

Also, p values indicate the effects of the considered terms of the model on the responses. The accuracy of the obtained model is evaluated by using the regression coefficients (R^2 and adjusted R^2) and the standard deviation (Eqs. (9)–(11)), to achieve the best response.

$$R^2 = 1 - \frac{\sum_{i=1}^{n}(y_i - \hat{y}_i)^2}{\sum_{i=1}^{n}(y_i - \bar{y})^2} \tag{9}$$

$$Adj\text{-}R^2 = 1 - \frac{(1 - R^2)(n - 1)}{(n - P - 1)} \tag{10}$$

$$Std.\ Dev. = \sqrt{\frac{\sum_{i=1}^{n}(y_i - \hat{y}_i)^2}{n - P}} \tag{11}$$

Here, y_i, $\hat{y}_i$, and $\bar{y}$ denote the experimental data, the predicted value by the model, and the average of experimental data, respectively. In addition, n and P are the numbers of experiments and predictors, respectively [24].

4 Results and Discussion

4.1 Characterization of Adsorbents

The elemental analysis related to the C, H, S, and N content of the prepared samples is summarized in Tab. 3. As can be observed, the carbon content is less than 25 % for all prepared samples, and the sum of C, H, S, and N does not reach the value of 30 % for each one, obtaining a remaining from the elemental analysis higher than 70 % that commonly is ascribed to the ashes and oxygen content. Also, the preparation of the samples shows a burn-off (weight loss) in consonance with the disappearance of volatile compounds and inorganic substances as consequence of the calcination and acid treatments, respectively, as reported in Tab. 4. More characterizations of samples are discussed in detail in Sect. S2 in the Supporting Information.

Table 3. Elemental analysis of the prepared samples.

Sample	C [%]	H [%]	S [%]	N [%]	Remaining [a] [%]	Ashes [b] [%]
CMSW-400	15.6	1.0	0.3	0.9	82.2	64.9
CMSW-800	17.5	0.4	0.4	0.0	81.6	80.6
CMSW-S	20.1	2.3	0.6	1.7	70.4	34.3
CMSW-S-800	20.5	1.9	0.4	1.4	75.8	65.9
CMSW-800-S	18.6	0.5	8.1	0.0	72.7	72.4

[a]Remaining was obtained from the subtraction of C, H, S, N, content from 100 %; [b]ashes values correspond with the weight of the samples at the end of the TGA in oxidizing atmosphere.

Table 4. Burn-off during the preparation of the prepared samples and textural properties of materials determined from BET and t-plot methods.

Sample	Burn-off [%]	S_{BET} [m²g⁻¹]	S_{ext} [m²g⁻¹]	S_{Mic} [m²g⁻¹]	V_{Mic} [mm³g⁻¹]	V_{Mic}/V_{Total} [%]	W_{Mic} [nm]
CMSW-400	23.9	22	22	0	0	0.0	0.0
CMSW-800	39.9	77	52	25	12	14.0	1.9
CMSW-S	59.6	11	11	0	0	0.0	–
CMSW-S-800	76.3	279	56	223	92	53.4	1.6
CMSW-800-S	58.7	91	60	31	14	13.6	1.8

4.2 Breakthrough Adsorption Evaluation

The breakthrough adsorption runs on the synthesized samples were performed at 40 °C and different pressures in the range of 1–5 bar. In this way, the inlet flow rate containing a specified percentage of CO_2 was fed to the fixed-bed column and the gas adsorption was started at the beginning of the column, i.e., the main region of the mass transfer zone (MTZ), on the fresh adsorbents until getting a saturation condition. Concerning the breakthrough curves, it should be considered that the ideal MTZ has no axial dispersion and no mass transfer resistance, which contributes to a short width, also a vertical line from 0 to 1.0. These behaviors can be observed in Figs. 5a–e. As shown, by increasing the total pressure from 1 to 5 bar, the MTZs are increased, which it can be interpreted by the reduction of the mass transfer rate because of the axial dispersion [25]. It is a worth mentioning that a shorter MTZ is favorable for the gas adsorption in the view of reduction of energy costs for the regeneration process [25].

The results of integration on the breakthrough curves by employing Eq. (1) contribute to the adsorption capacities of the samples [26]. The isotherm results of the prepared samples in this work are illustrated in Fig. 6a. As can be expected, the uptake capacities of all samples are increased by enhancing the pres-sure, which can be explained by Le Chatelier's principle, which considers the P_{CO_2} increment as a driving force for adsorption systems.

As previously mentioned, in this study the Langmuir model was applied to analyze and predict the isotherm results. In Fig. 6a the solid curves represent the results of the Langmuir model, and the marker points express the obtained experimental values. There is a good agreement between the experimental and modeling results, which demonstrates that this model is able to satisfactorily predict the behavior of the adsorption process. This is also confirmed by the Langmuir fitting results (R^2), which are reported in Tab. 5.

The uptake capacities of the prepared samples for CO_2 capture are compared in Fig. 6b. CMSW-S-800, which was subsequently treated chemically with sulfuric acid and then physically at 800 °C, has the highest uptake capacity, and CMSW-400 that was thermally activated at 400 °C, has the lowest adsorption capacity. To interpret the behaviors of these solid adsorbents, several factors should be taken into account. As can be expected, the chemical activation has a better effect than physical activation on the carbon-based materials for carbon capture [27]. Thus, CMSW-400 and CMSW-800 have lower adsorption capacities than other ones, and obviously the CMSW-800 sample due to the treatment at the higher temperature exhibits a better performance than the CMSW-400 sample.

On the other hand, based on the textural properties of the prepared samples (Tab. 4), CMSW-S-800 has the largest surface area compared to the other ones. Most of the adsorption occurs in these pores. CMSW-800-S is the other sample with high surface area, which is the next ideal adsorbent in this study. In addition, the higher uptake capacity of CMSW-S-800 can be also interpreted based on the consequence of the thermal treatment of this sample, which has been chemically activated in the previous step. Some of the functional groups, which are able to block the available pores, were removed and some new adsorption sites emerged. Thus, this sample shows a better performance for CO_2 adsorption. To have a better knowledge about the adsorption capacity of the best synthesized adsorbent (CMSW-S-800), a comparison with some of the recently studied sorbents for CO_2 capture is presented in Tab. 6.

Table 5. Langmuir parameters of CO_2 adsorption on prepared CMSW samples at 40 °C.

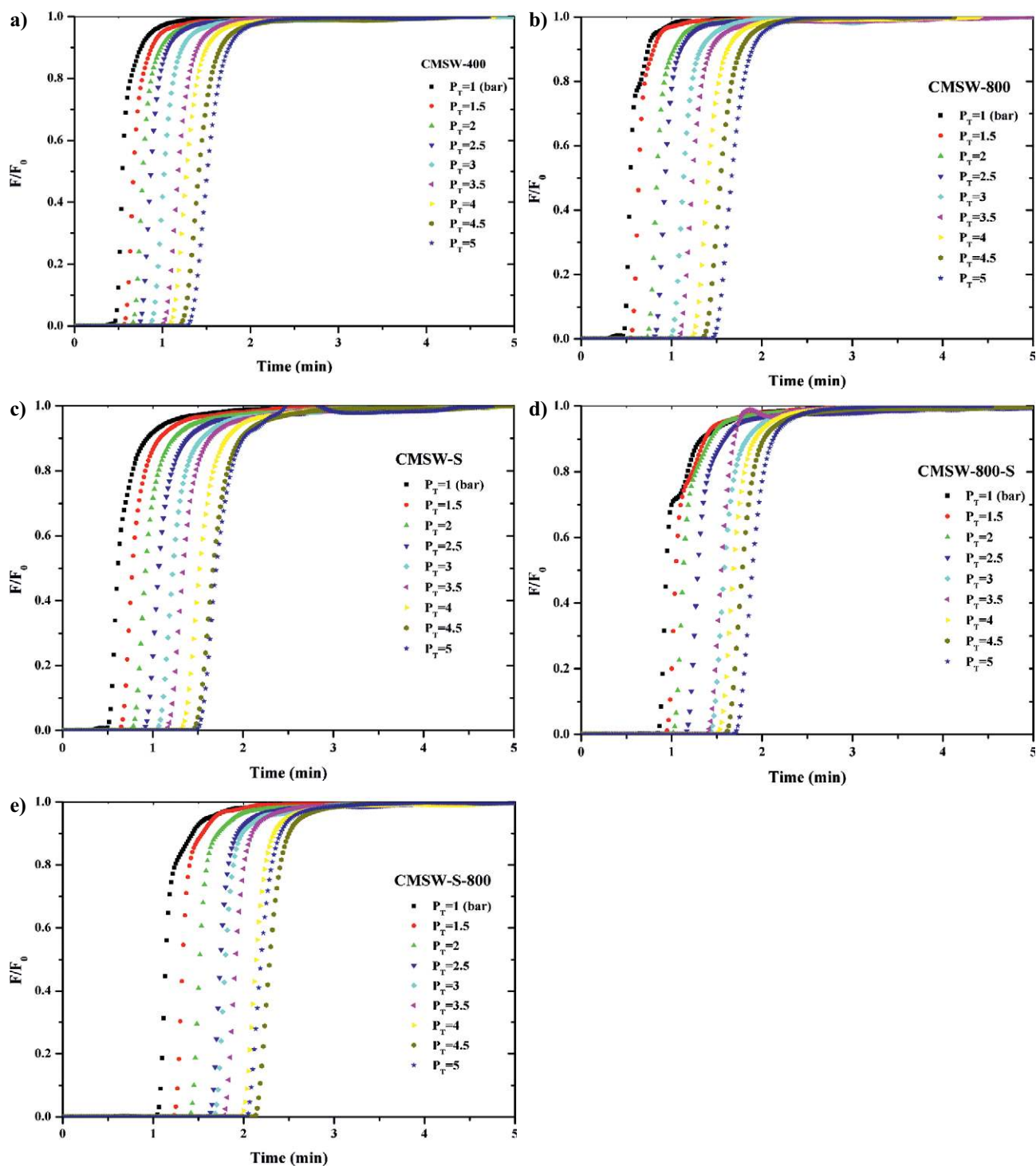| Langmuir coefficients	CMSW-400	CMSW-800	CMSW-S	CMSW-800-S	CMSW-S-800
Q_m [mmol g⁻¹]	2.09	2.31	2.26	2.67	3.29
K_L [bar⁻¹]	0.34	0.26	0.47	1.01	0.98
R^2	0.97	0.98	0.98	0.94	0.97

Figure 5. Breakthrough curves of adsorption measurements of CO_2 at 40 °C of (a) CMSW-400, (b) CMSW-800, (c) CMSW-S, (d) CMSW-800-S, (e) CMSW-S-800.

4.3 Central Composite Design Analysis

The adsorption of CO_2 on the newly developed adsorbents CMSW-S-800 and CMSW-800-S was assessed in the temperature range of 40–100 °C by applying the CCD as a design mod-el to the experimental runs [31–33]. The experimental values of input variables and their coded values, and also the response surfaces for CMSW-800-S and CMSW-S-800 samples are listed in Tab. 7.
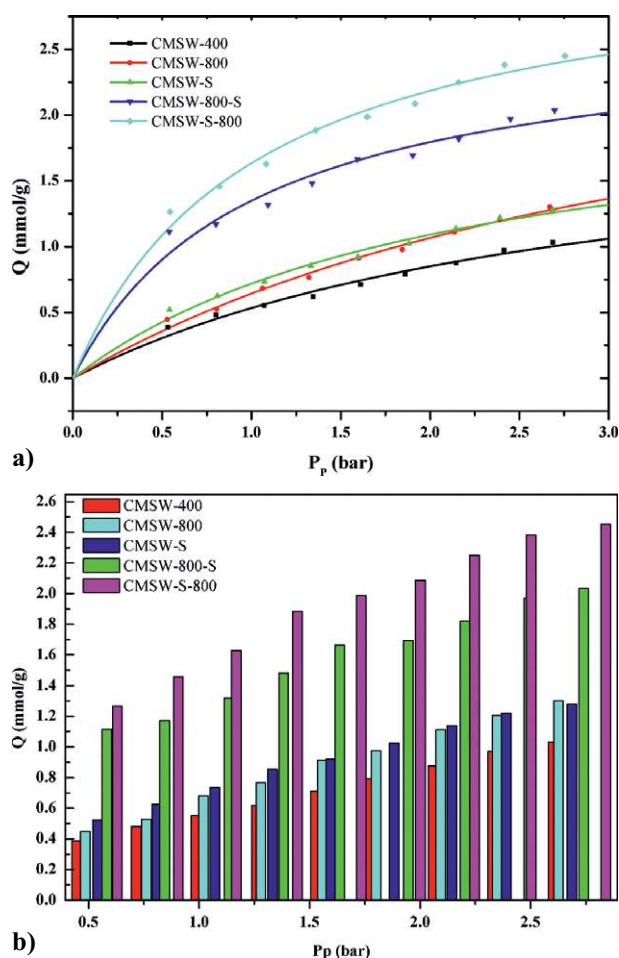
Chem. Eng. Technol. **2020**, *43*, No. 7, 1336–1349

© 2020 WILEY-VCH Verlag GmbH & Co. KGaA

www.cet-journal.com

Figure 6. (a) Experimental equilibrium data (symbols) and fitted Langmuir isotherm (lines) for CO_2 adsorption at 40 °C; (b) comparison between CO_2 uptake capacity (mmol g^{-1}) of investigated adsorbents.

The obtained experimental values were fitted with quadratic models to develop the general correlations for the uptake capacity and the breakthrough time of the specified samples. After that, the statistical analysis of models was carried out by employing the multiple regression analysis of ANOVA and considering the fitness of the models. In this regard, the significance of model and lack-of-fit, the coded coefficients, standard deviation, R^2, adjusted R^2 (Adj-R^2), and p values should be considered and analyzed. Then, the final models were developed after eliminating the insignificant interactions and parameters in the adsorption system. The ANOVA results of the employed polynomial models for the mentioned samples are summarized in Tabs. 8 and 9, respectively.

In addition, based on the regression analysis of ANOVA, the obtained response variables for the CMSW-800-S sample with non-coded values of T and P are as follows:

$$\left(Q_{CO_2}\right)_{CMSW\text{-}800S} = 1.73 + 0.796P - 0.03T$$
$$- (0.0035PT) - 0.045P^2$$
$$+ 0.00017T^2 \tag{12}$$

$$\left(t_b\right)_{CMSW\text{-}800S} = 2.92 + 0.398P - 0.02T - (0.0005PT)$$
$$+ 0.049P^2 + 0.00008T^2 \tag{13}$$

The uptake capacity and breakthrough time of the CMSW-S-800 sample are defined by the following equations:

$$\left(Q_{CO_2}\right)_{CMSW\text{-}S800} = 1.59 + 1.426P - 0.025T$$
$$- (0.001PT) - 0.247P^2$$
$$+ 0.0001T^2 \tag{14}$$

$$\left(t_b\right)_{CMSW\text{-}S800} = 3.069 + 1.136P - 0.02T - (0.0019PT)$$
$$- 0.163P^2 + 0.00007T^2 \tag{15}$$

Table 6. Comparison between the adsorption capacities of recent proposed adsorbents for CO_2 capture.

Adsorbent	Type of activation	$m_{adsorbant}$ [g]	Porosity	P_{CO2} [bar]	T [K]	Adsorption technique	Q [mmol g^{-1}]	Ref.
AC derived from coconut shell chars	Heat treatment at 250 °C	0.2	Microporous	2.5	273	Intelligent gravimetric analyzer (IGA)	1.5	[28]
	Heat treatment at 350 °C	0.2		2.5	273		2.15	
	Heat treatment at 450 °C	0.2		2.5	273		2.7	
	Heat treatment at 450 °C	0.2		2.5	273		3.6	
AC derived from pine sawdust	CO_2	4	Microporous	2.5	323	Magnetic suspension balance	2.8	[29]
MOF Fe(BTC)	Elevated by mixed- matrix membranes	–	Mesoporous	2.5	303	Thermogravimetric analysis (TGA)	1.5	[30]
				2.5	323		1.3	
				2.5	353		0.8	
AC (Norit R2030CO2)	Steam activation	3.22	Microporous	2	418	Breakthrough technique	2.5	[31]

Table 6. Continued

Adsorbent	Type of activation	$m_{adsorbant}$ [g]	Porosity	P_{CO_2} [bar]	T [K]	Adsorption technique	Q [mmol g^{-1}]	Ref.
Zeolite H-BETA-25	n/a	0.65	Micro-/meso-porous	2.5	313	Breakthrough technique	1.75	[32]
Zeolite H-BETA-150		0.65		2.5	313		1.67	
Zeolite Na-BETA-25		0.65		2.5	313		2.21	
AC derived from pine cone	H$_3$PO$_4$	–	Microporous	2.5	308	Volumetric technique	2.8	[33]
				2.5	318		2.1	
AC derived from cherry stones	CO$_2$	4.08	Microporous	2.5	323	Magnetic suspension balance	2.85	[34]
	Steam	4.8		2.5	323		2.5	
AHEP (algae)	KOH	0.7	Micro-/meso-porous	1	323	Breakthrough technique	0.413	[35]
AAM-silica	HCL	1	Micro-/meso-porous	1	318	Breakthrough technique	0.78	[36]
CMSW-800-S	Heat treatment at 800 °C and H$_2$SO$_4$	0.6	Mesoporous	2.5	313	Breakthrough technique	2.15	This Study
CMSW-S-800	H$_2$SO$_4$ and heat treatment at 800 °C	0.6	Mesoporous	2.5	313	Breakthrough technique	2.75	This Study

Table 7. Independent variables and response values for the considered CCD models of CMSW-800-S and CMSW-S-800 adsorbents; Total flow rate: 20 mL min^{-1}; mass of adsorbent: ~0.5 g; ambient temperature: 25 °C; ambient pressure: 1 bar; helium flow rate: ~8 mL min^{-1}.

Run	Independent variables		P_{CO_2} [bar]	CMSW-800-S		CMSW-S-800	
	T [°C]	P_{CO_2} [bar]		Q [mmol g^{-1}]	t_b [min]	Q [mmol g^{-1}]	t_b [min]
1	40 (−1)	0.5 (−1)	1	1.05	2.45	1.45	2.82
2	40 (−1)	1.5 (0)	3	1.75	2.95	2.15	3.65
3	40 (−1)	2.5 (+1)	5	2.15	3.46	2.75	3.95
4	70 (0)	0.5 (−1)	1	0.79	2.05	0.95	2.45
5	70 (0)	1.5 (0)	3	1.15	2.65	1.85	3.15
6	70 (0)	2.5 (+1)	5	1.47	3.15	2.15	3.50
7	100 (+1)	0.5 (−1)	1	0.66	1.95	0.77	2.15
8	100 (+1)	1.5 (0)	3	0.91	2.3	1.65	2.75
9	100 (+1)	2.5 (+1)	5	1.33	2.9	1.95	3.05
10	70 (0)	1.5 (0)	3	1.05	2.45	2.05	3.05
11	70 (0)	1.5 (0)	3	1.22	2.60	1.73	2.95
12	70 (0)	1.5 (0)	3	1.35	2.73	1.92	3.10
13	70 (0)	1.5 (0)	3	1.17	2.40	1.80	3.23

According to the ANOVA results (Tabs. 8 and 9), all developed models are statistically significant, since the p value is < 0.0001, by having non-significant lack of fits, which are the main factors of an authentic model. The proposed models for

CO$_2$ uptake capacity and breakthrough time exhibit acceptable values for the standard deviation, R^2, and $Adj\text{-}R^2$ which indicate that the considered values fit properly the developed models, and they have an excellent capacity to predict the response surfaces under other required operational conditions.

On the other hand, by evaluation of coded coefficients, it can be revealed that the linear coefficients exert stronger effects on the adsorption process than other ones, by having −0.34 and 0.41 for $(Q_{CO_2})_{CMSW-800S}$, −0.29 and 0.51 for $(t_b)_{CMSW-800S}$, −0.33 and 0.61 for $(Q_{CO_2})_{CMSW-S800}$, and −0.41 and 0.51 for $(t_b)_{CMSW-S800}$ responses, respectively, for linear temperature and pressure coefficients. Furthermore, it can be stated that among the linear variables the adsorption pressure is the determinative one. Here, the negative values of the linear coefficients of temperature (−0.34, −0.29, −0.33, and −0.41 for $(Q_{CO_2})_{CMSW-800S}$, $(t_b)_{CMSW-800S}$, $(Q_{CO_2})_{CMSW-S800}$, and $(t_b)_{CMSW-S800}$ responses, respectively) express a negative effect of temperature increase, while the positive values of pressure, in accordance with the Le Chatelier's principle, illustrate the constructive effect of pressure increment on the adsorption process.

In addition, the ANOVA results demonstrate that the interaction effects of $(Q_{CO_2})_{CMSW-800S}$ are significant (coded coeffi-

Table 8. Analysis of variance (ANOVA) of CCD for CO_2 adsorption and breakthrough time on CMSW-800-S.

	Coded coefficient	Standard error	Sum of squares	Mean squares	df	p value
CO_2 uptake capacity Q [mmol g^{-1}]						
Model			1.81	0.36	5	0.0001
T	−0.34	0.044	0.70	0.70	1	0.0001
P_{CO_2}	0.41	0.044	1.00	1.00	1	<0.0001
TP_{CO_2}	−0.11	0.054	0.046	0.046	1	0.0857
T^2	0.15	0.065	0.066	0.066	1	0.0485
$P_{CO2}{}^2$	−0.046	0.065	0.005	0.005	1	0.5029
Residual			0.081	0.012	7	
Lack-of-fit			0.033	0.011	3	0.5108
Pure error			0.048	0.012	4	
Total			1.89		12	
Std. dev.	0.11					
R^2	0.957					
Adj-R^2	0.927					
Breakthrough time t_b [min]						
Model			2.08	0.42	5	<0.0001
T	−0.29	0.045	0.49	0.49	1	0.0004
P_{CO_2}	0.51	0.043	1.56	1.56	1	<0.0001
TP_{CO_2}	−0.015	0.056	0.0009	0.0009	1	0.7949
T^2	0.074	0.067	0.015	0.015	1	0.3051
$P_{CO2}{}^2$	0.049	0.066	0.007	0.007	1	0.4876
Residual			0.086	0.012	7	–
Lack-of-fit			0.01	0.003	3	
Pure error			0.076	0.019	4	
Total			2.17		12	
Std. dev.	0.11					
R^2	0.960					
Adj-R^2	0.932					

$$\left(Q_{CO_2}\right)_{\text{CMSW-800S}} = 1.73 + 0.796P - 0.03T - (0.0035PT) + 0.00017T^2 \quad (16)$$

$$\left(t_b\right)_{\text{CMSW-800S}} = 2.92 + 0.398P - 0.02T \quad (17)$$

In a same trend, the evaluation of second-order coefficients of the CMSW-S-800 sample illustrates that the adsorption temperature is not statistically significant in Q and t_b models (p value 0.1875 and 0.2786 for $(Q_{CO2})_{\text{CMSW-S800}}$ and $(t_b)_{\text{CMSW-S800}}$, respectively); thus, to increase the confidence level of the obtained models to more than 0.95, these terms can be eliminated from Eqs. (14) and (15), and they are also simplified as:

$$\left(Q_{CO_2}\right)_{\text{CMSW-S800}} = 1.59 + 1.426P - 0.025T - 0.247P^2 \quad (18)$$

$$\left(t_b\right)_{\text{CMSW-S800}} = 3.069 + 1.136P - 0.02T - 0.163P^2 \quad (19)$$

To describe the characteristics of the adsorption systems, the obtained results of the CCD models for the CMSW-800-S and CMSW-S-800 samples are depicted in Figs. 7 and 8. As can be expected, the uptake capacity of both samples was improved by increasing the adsorption pressure (Figs. 7a and 8a), while the temperature increment had a negative effect on the adsorption process. A same trend can be observed for the breakthrough time (Figs. 7b and 8b). On the other hand, as can be observed, the breakthrough time of the CMSW-800-S sample has (almost) a linear behavior according to the significant order of the different variables (ANOVA results).

cients: −0.11, p value: 0.0857), while this parameter is negligible for other response surfaces (including −0.015, −0.03, and −0.057 for $(t_b)_{\text{CMSW-800S}}$, $(Q_{CO2})_{\text{CMSW-S800}}$, $(t_b)_{\text{CMSW-S800}}$, respectively). Also, the analysis of second-order coefficients for the CMSW-800-S sample indicates that the temperature is the only significant parameter for CO_2 capture capacity, and the other ones are negligible to achieving models with more than 0.95 confidence levels. Thus, Eqs. (12) and (13) can be simplified as:

Table 9. Analysis of variance (ANOVA) of CCD for CO_2 adsorption and breakthrough time on CMSW-S-800.

	Coded coefficient	Standard error	Sum of squares	Mean squares	df	p value
CO_2 uptake capacity Q [mmol g^{-1}]						
Model			3.08	0.62	5	< 0.0001
T	−0.33	0.048	0.65	0.65	1	0.0002
P_{CO_2}	0.61	0.048	2.26	2.26	1	<0.0001
TP_{CO_2}	−0.03	0.058	0.003	0.003	1	0.6225
T^2	0.10	0.070	0.029	0.029	1	0.1875
$P_{CO_2}^2$	−0.25	0.070	0.17	0.17	1	0.0096
Residual			0.095	0.014	7	
Lack-of-fit			0.035	0.012	3	0.5610
Pure error			0.060	0.015	4	
Total			3.18		12	
Std. dev.	0.12					
R^2	0.971					
Adj-R^2	0.948					
Breakthrough time t_b [min]						
Model			2.68	0.54	5	< 0.0001
T	−0.41	0.036	1.02	1.02	1	< 0.0001
P_{CO_2}	0.51	0.036	1.58	1.58	1	< 0.0001
TP_{CO_2}	−0.057	0.044	0.013	0.013	1	0.2329
T^2	0.062	0.053	0.011	0.011	1	0.2786
$P_{CO_2}^2$	−0.16	0.053	0.073	0.073	1	0.0180
Residual			0.054	0.007	7	–
Lack-of-fit			0.009	0.003	3	
Pure error			0.044	0.011	4	
Total			2.74		12	
Std. dev.	0.088					
R^2	0.981					
Adj-R^2	0.966					

was 2.5 mmol g^{-1} at 2.5 bar and 40 °C (around 11 wt %), which is in the range of commercial carbon materials.

In the next step, statistical analysis and adsorption performance of the best samples were performed by means of the CCD technique and RSM strategy. It revealed that the CO_2 partial pressure and the adsorption temperature are the main factors in the adsorption process. Finally, by considering the worldwide abundance of municipal solid wastes, this study can be considered as a green route for the solid wastes management and carbon capture and storage.

Acknowledgment

The authors have declared no conflict of interest.

5 Conclusion

The potential of compost derived from municipal solid wastes as a low-cost source of adsorbents for CO_2 capture was investigated. Five different samples were synthesized and screened regarding the CO_2 uptake. The breakthrough results showed that the CMSW-S-800, which was chemically treated by sulfuric acid and thermally activated at 800 °C, had the highest breakthrough time of around 4 min and its adsorption capacity

Supporting Information

Supporting Information for this article can be found under DOI: https://doi.org/10.1002/ceat.201900108.
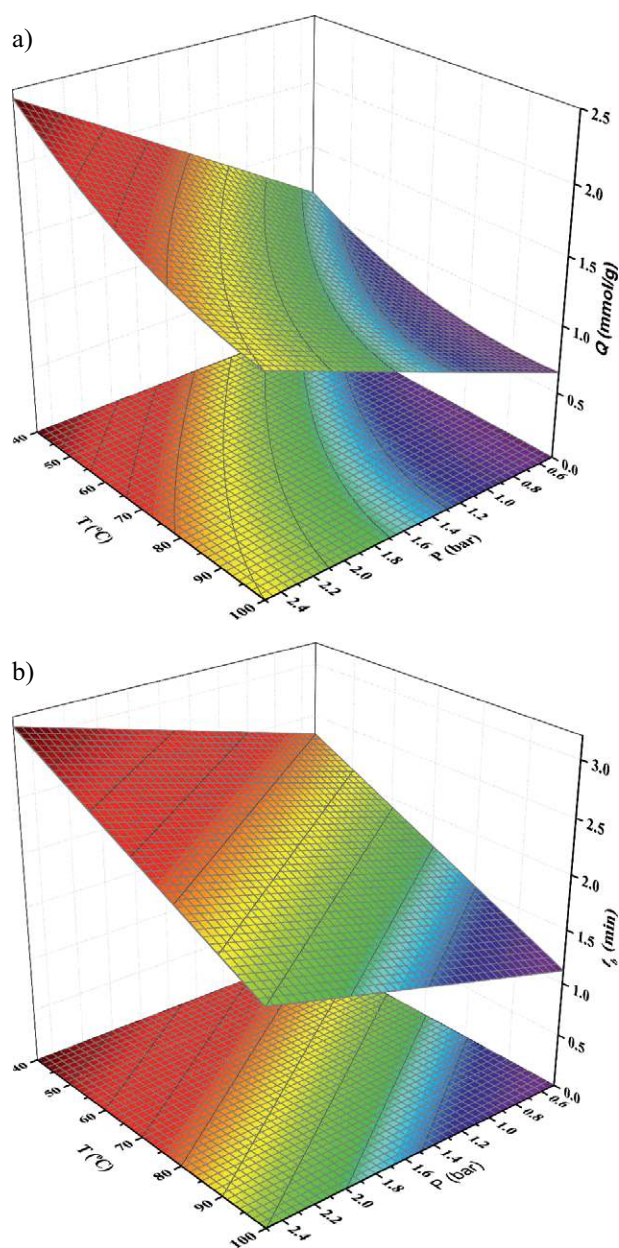
a)

b)

Figure 7. Response surface of (a) CO_2 uptake capacity of CMSW-800-S sample, (b) breakthrough time (t_b) as a function of adsorption pressure and temperature.
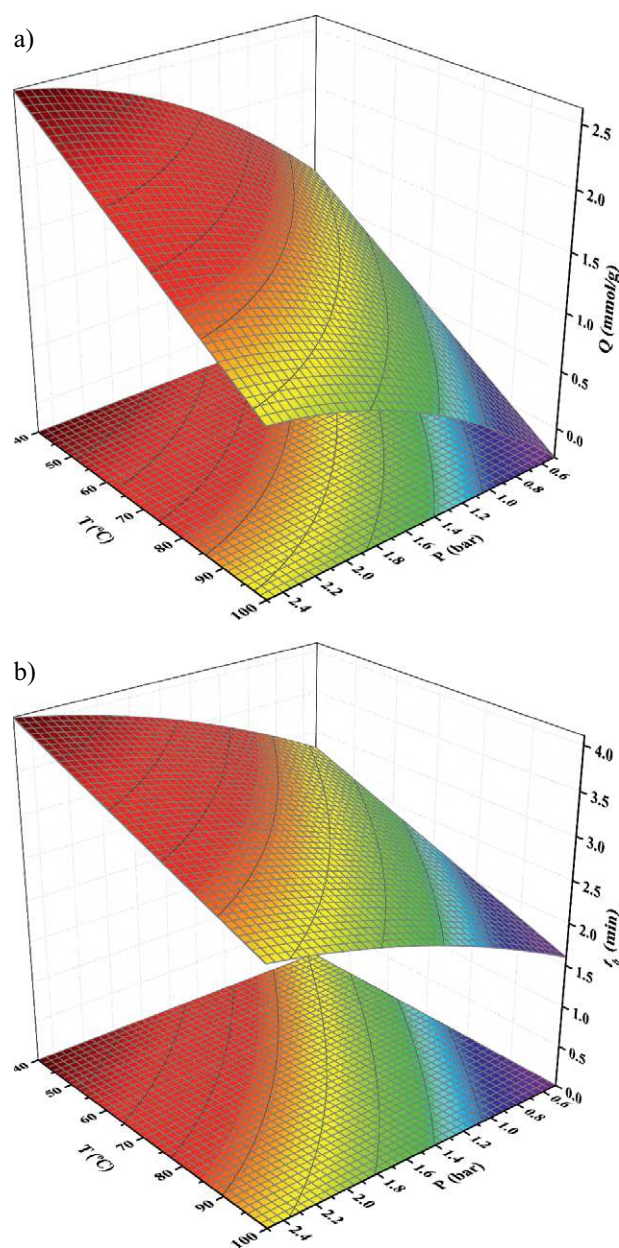
a)

b)

Figure 8. Response surface of (a) CO_2 uptake capacity of CMSW-S-800 sample, (b) breakthrough time (t_b) as a function of adsorption pressure and temperature.

Symbols used

D_{microp}	[mm]	average pore diameter
$F_{CO_2,in}$	[mL min^{-1}]	molar flow rate of CO_2 at the bed inlet
$F_{CO_2,out}$	[mL min^{-1}]	molar flow rate of CO_2 at the bed outlet
ΔH	[kJ mol^{-1}]	heat of adsorption
K_L	[bar^{-1}]	Langmuir adsorption constant
K_∞	[bar^{-1}]	affinity constant
M	[g mmol^{-1}]	molecular weight
$m_{adsorbent}$	[g]	mass of adsorbent in the bed
P_b	[bar]	pressure of bed at equilibrium
P_{CO2}	[bar]	partial pressure of CO_2
Q_e	[mmol g^{-1}]	adsorption capacity at equilibrium condition
Q_m	[mmol g^{-1}]	maximum adsorption capacity
S_{BET}	[m^{2}g^{-1}]	specific surface area
S_{ext}	[m^{2}g^{-1}]	external surface area
S_{Mic}	[m^{2}g^{-1}]	microporous surface area
t_b	[min]	breakthrough time

t_s	[min]	saturation time
T_b	[K]	temperature of bed at equilibrium
V_b	[cm^3]	bed volume
V_d	[cm^3]	dead volume
V_{Mic}	[mm^{3}g^{-1}]	micropore volume
V_{Total}	[mm^3]	total pore volume
W_{Mic}	[nm]	width of micropore
$y_{CO_2,feed}$	[–]	molar fraction of CO_2 in feed stream
Z	[–]	CO_2 compressibility factor at P_b and T_b

Greek letters

α	[–]	sticking coefficient
ε	[–]	residual error
ε_b	[–]	packed bed porosity
ε_P	[–]	particle porosity
ε_T	[–]	total porosity of bed

Subscripts and superscripts

Ads.	adsorbent
min	minute
Tot	total

Abbreviations

ANOVA	analysis of variance
BET	Brunauer-Emmett-Teller
CCD	central composite design
GHG	greenhouse gas
IME	integrated management of environment
MSW	municipal solid waste
MTZ	mass transfer zone
RSM	response surface methodology
TCD	thermal conductivity detector
TGA	thermogravimetric analysis

References

[1] M. Karimi, M. R. Rahimpour, R. Rafiei, M. Jafari, D. Iranshahi, A. Shariati, *J. Nat. Gas Sci. Eng.* **2014**, *17*, 136–150.

[2] *CO₂ Emissions from Fuel Combustion*, International Energy Agency (IEA), Paris **2014**. DOI: https://doi.org/10.1787/co2_fuel-2014-en

[3] *Climate Change 2013: The Physical Science Basis. Contribution of Working Group I to the Fifth Assessment Report of the Intergovernmental Panel on Climate Change* (Eds: T. F. Stocker, D. Qin, G. K. Plattner, M. Tignor, S. K. Allen, J. Boschung, A. Nauels, Y. Xia, V. Bex, P. M. Midgley), Cambridge University Press, New York **2013**.

[4] D. Iranshahi, M. Karimi, S. Amiri, M. Jafari, R. Rafiei, M. R. Rahimpour, *Chem. Eng. Res. Des.* **2014**, *92 (9)*, 1704–1727.

[5] M. Karimi, M. R. Rahimpour, D. Iranshahi, *Chem. Eng. Technol.* **2018**, *41 (9)*, 1746–1758.

[6] M. Karimi, M. R. Rahimpour, R. Rafiei, A. Shariati, D. Iranshahi, *Appl. Therm. Eng.* **2016**, *94*, 543–558.

[7] M. Shirzad, M. Karimi, J. A. C. Silva, A. E. Rodrigues, *Ind. Eng. Chem. Res.* **2019**, *58 (22)*, 9179–9198.

[8] C. Zhao, X. Chen, C. Zhao, *Energy Fuels* **2012**, *26*, 1401–1405.

[9] M. Karimi, J. A. C. Silva, C. N. d. P. Gonçalves, J. L. Diaz de Tuesta, A. E. Rodrigues, H. T. Gomes, *Ind. Eng. Chem. Res.* **2018**, *57 (32)*, 11154–11166.

[10] J. A. Mason, T. M. McDonald, T. H. Bae, J. E. Bachman, K. Sumida, J. J. Dutton, S. S. Kaye, J. R. Long, *J. Am. Chem. Soc.* **2015**, *137 (14)*, 4787–4803.

[11] R. Wennersten, Q. Sun, H. Li, *J. Cleaner Prod.* **2014**, *103*, 724–736.

[12] T. Karak, R. M. Bhagat, P. Bhattacharyya, *Crit. Rev. Environ. Sci. Technol.* **2012**, *42 (15)*, 1509–1630.

[13] *Solid Waste Management, United Nations Environment Program* (Eds: L. F. Diaz, P. Bakken), Vol. I, CalRecovery, Inc., Concord, CA **2005**.

[14] *A Global Snapshot of Solid Waste Management to 2050* (Eds: S. Kaza, L. Yao, P. Bhada-Tata, F. V. Woerden), The World Bank, Washington, D.C. **2018**.

[15] *Handbook of Solid Waste Management* (Eds: G. Tchobanoglous, F. Kreith), 2nd ed. McGraw Hill, New York **2002**.

[16] S. Brunauer, P. H. Emmett, E. Teller, *J. Am. Chem. Soc.* **1938**, *60 (2)*, 309–319.

[17] B. C. Lippens, J. H. de Boer, *J. Catal.* **1965**, *4*, 319–323.

[18] J. A. C. Silva, K. Schumann, A. E. Rodrigues, *Microporous Mesoporous Mater.* **2012**, *158*, 219–228.

[19] J. M. Becnel, C. E. Holland, J. McIntyre, M. A. Matthews, J. A. Ritter, *American Society for Engineering Education Annual Conference & Exposition*, Montréal, QC **2002**.

[20] J. A. C. Silva, A. E. Rodrigues, *Chem. Eng. Technol.* **2015**, *38 (12)*, 2335–2339.

[21] I. Langmuir, *J. Am. Chem. Soc.* **1916**, *38 (11)*, 2221–2295.

[22] *Response Surface Methodology: Process and Product Optimization Using Designed Experiments* (Eds: R. H. Myers, D. C. Montgomery, C. M. Anderson-Cook), 4th ed. John Wiley & Sons, Hoboken, NJ **2016**.

[23] S. García, M. V. Gil, J. J. Pis, F. Rubiera, C. Pevida, *Int. J. Greenhouse Gas Control* **2013**, *12*, 35–43.

[24] T. Z. E. Lee, C. Krongchai, N. A. L. M. Irwn Lu, S. Kittiwachana, S. F. Sim, *Int. J. Ind. Chem.* **2015**, *6*, 185–191.

[25] *Unit Operations of Chemical Engineering* (Eds: W. L. McCabe, J. C. Smith, P. Harriott), 7th ed. McGraw-Hill, New York **2005**.

[26] L. K. G. Bhatta, S. Subramanyam, M. D. Chengala, S. Olivera, K. Venkatesh, *J. Cleaner Prod.* **2015**, *103*, 171–196.

[27] S. Shahkarami, R. Azargohar, A. K. Dalai, J. Soltan, *J. Environ. Sci.* **2015**, *34*, 68–76.

[28] C. Tangsathitkulchai, S. Junpirom, J. Katesa, *J. Nanomater.* **2016**, *2016*, 4292316.

[29] I. Durán, N. Álvarez-Gutiérrez, F. Rubiera, C. Pevida, *Chem. Eng. J.* **2018**, *353*, 197–207.

[30] A. R. Nabais, R. P. P. L. Ribeiro, J. P. B. Mota, V. D. Alves, I. A. A. C. Esteves, L. A. Neves, *Sep. Purif. Technol.* **2018**, *202*, 174–184.

[31]   S. García, M. V. Gil, C. F. Martín, J. J. Pis, F. Rubiera, C. Pevida, *Chem. Eng. J.* **2011**, *171*, 549–556.

[32]   A. Henrique, M. Karimi, J. A. C. Silva, A. E. Rodrigues, *Chem. Eng. Technol.* **2019**, *42 (2)*, 327–342.

[33]   S. Khalili, B. Khoshandam, M. Jahanshahi, *RSC Adv.* **2015**, *5*, 94115–94129.

[34]   N. Álvarez-Gutiérrez, M. V. Gil, F. Rubiera, C. Pevida, *Fuel Process. Technol.* **2016**, *142*, 361–369.

[35]   Z. Zhang, K. Wang, J. D. Atkinson, X. Yan, X. Li, M. J. Rood, Z. Yan, *J. Hazard. Mater.* **2012**, *229*, 183–191.

[36]   Y. Zhao, Y. Shen, L. Bai, S. Ni, *Appl. Surf. Sci.* **2012**, *261*, 708–716.